

REDUCING THE LEWIS ACIDITY AT THE METAL CENTER OF IRON(II) COMPLEXES WITH TPA LIGANDS BY ADDING AN ELECTRON-DONATING SUBSTITUTION

Dr. NASSER THALLAJ

Assistant Professor, Pharmaceutical chemistry and Drug Quality Control Department, Faculty of Pharmacy, Al-Rachid privet University, Damascus, Syria.

ABSTRACT

Biomimetic oxidations at active sites of iron proteins involve peroxides, particularly hydrogen peroxide, which is a powerful and very convenient reagent as it is inexpensive and does not release toxic by-products. In many cases, however, Mother Nature uses molecular oxygen to carry out large-scale oxidation reactions under particularly attractive conditions. The biomimetic interest of iron complexes of the tris(2-pyridylmethyl)amine series (TPA) can no longer be proven. We have prepared various -substituted TPA-based ligands with the idea of modulating the electronic properties at the metal center. We prepared the new type of ligand MeOTPA and studied the effect of (MeO) on the oxygenation of the complex.

Keywords: Biomimetic, electron-donatin, tris (2-pyridylmethyl) amine, iron^(II)complex, dioxygen activation.

I- Introduction

The catalysis of oxygen transfer to organic substrates is well known in biology and can be performed by enzymes encoding metalloproteins with a heme-type (e.g. cytochrome P-450) or non-heme (e.g. methane monooxygenase) [1]. These reactions can be carried out using molecular oxygen. In this case it must be fixed. Then either formation of a hydroperoxo-reactive species or cleavage of the O-O bond can occur. In the latter case, highly reactive metal oxo compounds are formed [2]. Iron complexes with tris(2-pyridylmethyl)amine (TPA) tetradent ligands and some of its derivatives have been well studied over the last twenty years. Some of them show functional analogies to certain non-heme iron enzymes involved in oxygen activation [3]. In most cases, however, hydroperoxides are used as oxygen donors [4-7]. However, molecular oxygen has been put to good use, but only reacts with iron compounds that are already coordinated with substrates that activate the metal, such as B. catechins or thiolates [8-10]. The investigation of a series of dichloroiron(II) complexes with substituted TPA-type ligands has been carried out in the laboratory [11-12]. At the ligand, substitution of nitrogen can induce three-point coordination of the ligand (potentially four-point). The complexes formed in this way can react with molecular oxygen without any special activation, provided the ligand is substituted by halogens. So there is a double effect here, steric and electronic. One of our goals is to build artificial systems that are active for molecular oxygen. Ideally, this requires the presence of an oxygen binding site, an electron source (external or grafted), and a site protection matrix, the latter of the protein type (eg, riboflavin or nanotube). In any case,

it is important to have a set of functional complexes that also have interesting reactivity. This is the context in which this study is set.

First, we prepared ligands with TPA structure monosubstituted by functional groups and added them to our series of this type of ligands [13–22] studied previously. Their synthesis is described. We then present the coordination chemistry of these ligands, which we approach through the preparation of dichloroiron(II) complexes[22–36]. One of the complexes produced was fully characterized and studied in solution. Finally, we describe the first studies on the reactivity of this complex towards molecular oxygen. Following the same lines of thought, we wanted to study complexes coordinated with ligands substituted by groups known as electron donors. This is how the preparations of the methoxy-substituted ligand complexes discussed for the first time in this work arose.

II-Synthesis of ligand MeOTPA

The MeOTPA ligands are synthesized using standard laboratory procedures, the synthesis of a monosubstituted tris(2-pyridylmethyl)amine (TPA) ligand is a second-order nucleophilic substitution reaction carried out starting from bis(2-pyridylmethyl)amine (DPA) and the appropriate brominated reagent, here 6-methoxy-2-bromomethylpyridine, in the presence of a base. Implementation in acetonitrile according to (Figure .1). Depending on the case, the products are white to yellow-orange in color and are generally obtained in yields of between 80 and 85%. They are generally characterized by 1 H NMR, 13 C and elemental analysis.

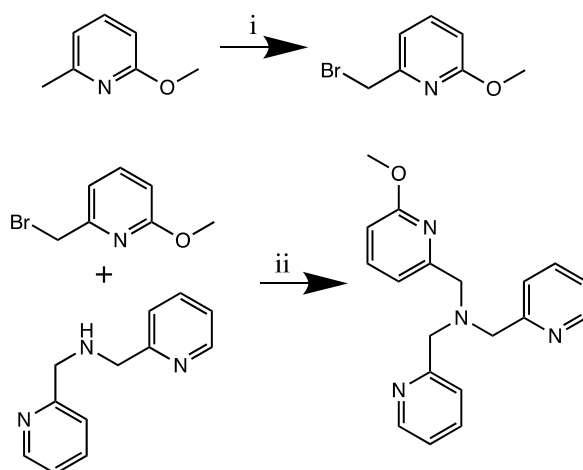
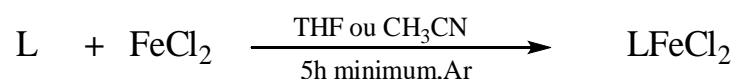


Figure1: i): NBS, AIBN, CCl₄, reflux 15h for, ii): Na₂CO₃ in CH₃CN reflux for 16h.

III-Complexation of (MeO)TPA:

The ligands whose synthesis is described above were metallated with anhydrous ferrous chloride specially prepared for this purpose in the laboratory. Indeed, commercial ferrous chloride is very often hydrated and contaminated with small amounts of ferric salts, which give it a pale brown color at best. Anhydrous FeCl₂ is an entirely white solid



The generic reaction is very simple and involves the use of one equivalent of ligand relative to the metal salt under strictly anhydrous conditions and under an argon atmosphere. The solvents are therefore freshly distilled using appropriate desiccants and subjected to extensive cryogenic degassing before use. The methodology used is that known as the Schlenck technique. Basically and for practical reasons of further processing, a 10% ligand excess speaks against iron(II) chloride. The yields of pure isolated products are generally between 80 and 90%. It is very likely that the reaction is quantitative, but more or less important amounts of compound are lost during the treatment, which here is carried out entirely under an inert atmosphere. In the solid state, the compounds z. B. with an inverted argon funnel for a few seconds quickly handled from the Schlenck tube.

The solids obtained are generally sufficiently soluble in nitriles to be assayed in solution in this type of solvent. The methodology used for their characterization is simple and consists of using the following techniques: UV-visible absorption spectroscopy.; Paramagnetic Nuclear Magnetic Resonance; Electrochemical measurements: conductimetry.; X-ray diffraction on single crystals when possible.

UV- visible and conductimetry

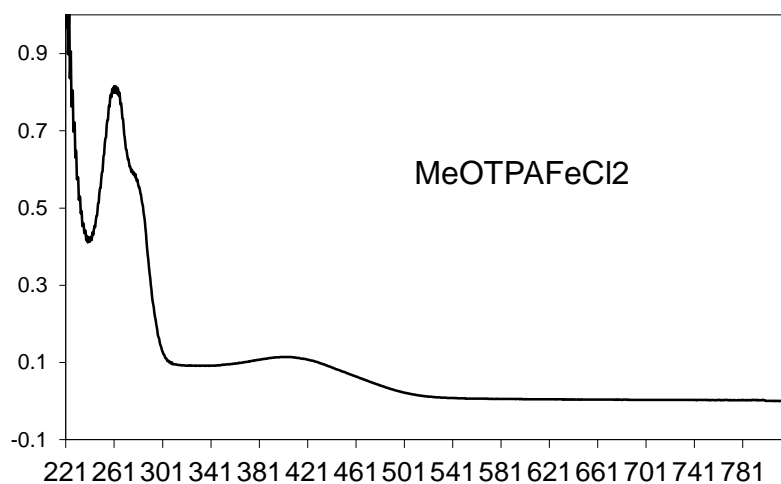


Figure II: The UV-visible spectrum for the MeOTPAFeCl₂ complex.

The presence of a well-defined MLCT-type absorption (Table I) at $\lambda = 403$ nm with a relatively strong intensity ($\epsilon = 1652.1$ mmol⁻¹ cm²) strongly suggests a tetradentate coordination mode for this ligand (Figure II), at which the three involved are pyridines [11-22].

UV-visible, λ , nm (ϵ , mmmol ⁻¹ .cm ²)		conductimetry
$\lambda \Rightarrow \lambda^*$	<u>MLCT</u>	Λ , S.mol ⁻¹ .cm ²
262.0 (11767.2)	403.5 (1652.1)	24.62

Table I: the value of absorption in UV- visible spectrum and the conductimetry of complex MeOTPAFeCl₂ .

¹H RMN :

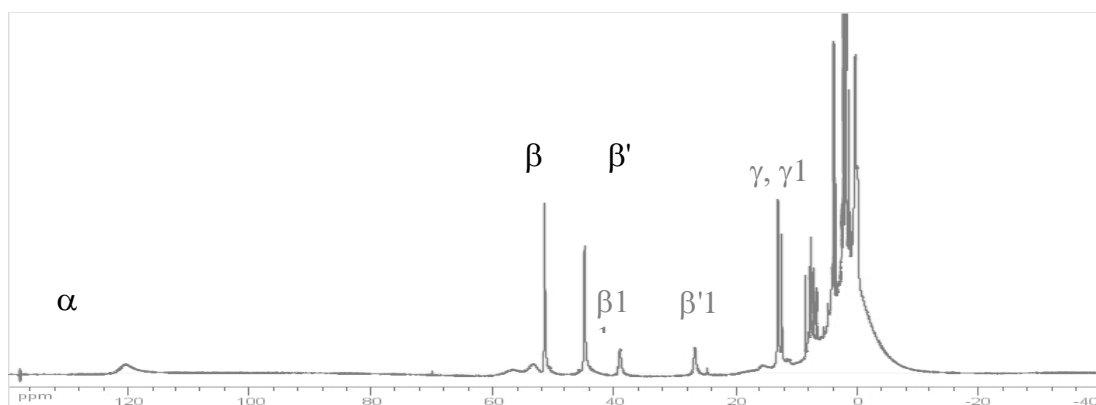


Figure III : The ¹H NMR spectrum for the MeOTPAFeCl₂ complex.

This spectrum is characteristic of a strong-spin Fe^(III) species with pseudooctahedral geometry in which the ligands are tetradentally coordinated [11,22]: the two subtle and intense signals correspond to the α and α' protons of non-pyridines. replaced (Figure III); those with weaker intensity, to protons β and β' to substituted pyridine. It can also be compared with the spectra of the derivatives of the mono- and difluorinated ligands described in Chapter 4. The methylene protons appear as broad peaks between 40 and 60 ppm.

Radiocrystallographic structure

Crystallization of the solid originating from the metallation of the ligand was carried out by the usual methods under an inert atmosphere. We get the following parameters: Triclinic system, space group P-1. Mesh parameters: $a = 89.7860(9)$ Å, $b = 10.4530(10)$ Å, $c = 11.0840(15)$ Å, $\alpha = 65.887(3)^\circ$, $\beta = 78.897(4)^\circ$, $\gamma = 71.118(3)^\circ$. $Z = 1$, $V = 976.80(19)$ Å³. A Mercury diagram is shown in Figure VI. Surprisingly, the compound which crystallizes is the μ -dichloro-bridged binuclear complex. The ligand coordinates here tridentally, the decoordinates arm being the one superseded by the methoxyl function. The main metal-ligand distances and angles are given in TableII.

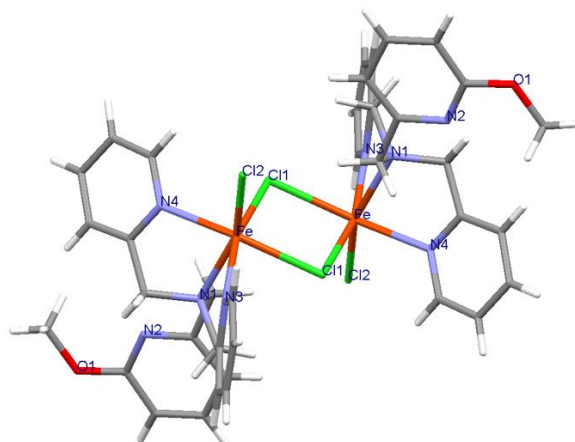


Figure IV: Mercury representation of the metallation product of (MeO) TPA by FeCl₂.

MeOTPAFeCl₂	
<u>Distances</u>	<u>Angles</u>
Fe-N3 2.215(2)Å	N3 Fe N4 109.25(9)°
Fe-N4 2.233(2)Å	N3 Fe N1 73.72(8)°
Fe-N1 2.316(2)Å	N4 Fe N1 74.07(8)°
Fe-Cl2 2.3612(8)Å	N3 Fe Cl2 95.30(6)°
Fe-Cl1 2.4986(8)Å	N4 Fe Cl2 91.50(6)°
Fe-Cl1 2.5091(8)Å	N1 Fe Cl2 157.15(6)°
Cl1-Fe 2.5091(8)Å	N3 Fe Cl1 82.11(6)°
Fe-Fe=3.789 Å	N4 Fe Cl1 157.32(7)°
	N1 Fe Cl1 91.26(6)°
	Cl2 Fe Cl1 107.31(3)°
	N3 Fe Cl1 161.85(6)°
	N4 Fe Cl1 83.51(7)°
	N1 Fe Cl1 98.54(6)°
	Cl2 Fe Cl1 97.25(3)°
	Cl1 Fe Cl1 81.67(3)°
	Fe Cl1 Fe 98.33(3)°

Table II: Main metal-ligand distances and angles.

Obtaining such a structure really surprised us: UV-visible spectroscopy clearly shows the tetradent character of the ligand; ¹H NMR shows a very usual spectrum in which the protons □ and □ appear to belong to the substituted pyridine bound to the metal. Molar conductimetry is not very informative: both the presumed mononuclear species in solution and the crystalline product are neutral. We must try to explain this structure: a methoxy function is not larger than a bromine atom, but we know that in the latter case a mononuclear is obtained [11]. It can be argued that the pyridine substituted by a methoxy group, which is richer in electrons, is less acceptor than a simple pyridine, and that its coordination to a discontinued metal could be less favored.

The thermodynamically stable product obtained after a few days of crystallization would be the binuclear complex of octahedral geometry with μ -dichloro bridge.

Oxygenation of (MeO) TPAFeCl₂.

UV-visible tracking

It is easy to see that the oxygenation reaction of (MeO) TPAFeCl₂ is slow and gradual. The spectrum no longer changes after about 20 hours, and the absorptions observed at $\lambda = 332$ nm and $\lambda = 390$ nm are characteristic of the presence of a diferric μ -oxo species of symmetrical structure. Figure V reports the observed spectroscopic changes.

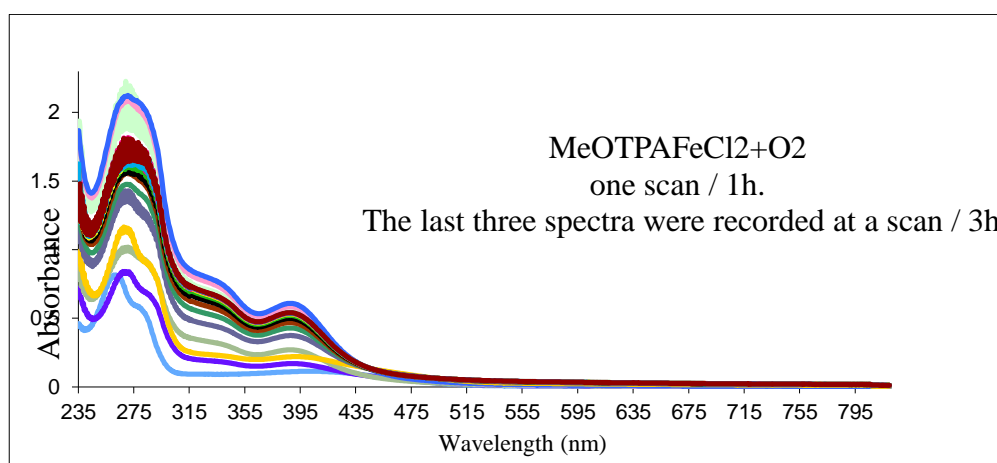


Figure V: Monitoring by UV-visible spectroscopy of the oxygenation reaction of the MeOTPAFeCl₂ complex.

1H NMR data

We did not record full kinetics for this reaction. Let's just say after 36 hours no more starting material is detected in the tube. The main signals of the final product appear between $\delta = 5$ and 35 ppm and exhibit large line widths. The cropping of the observation window and the large width at half height suggests the presence of a ferric entity whose ground state approaches a diamagnetic state (Figure VI).

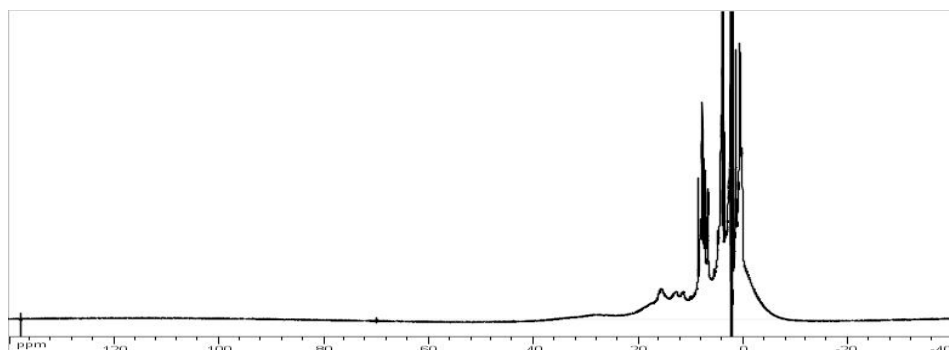


Figure VI: The ^1H NMR spectrum of the oxygenation reaction product of the (MeO)TPAFeCl₂ complex.

Structure of the final compound

An oxygenated solution of the starting material was covered with diethyl ether. After a few days, single crystals appeared, and the radiocrystallographic structure could be resolved. Here are the mesh parameters:

Triclinic system, space group P-1. $a = 9.8800(11) \text{ \AA}$, $b = 10.1200(13) \text{ \AA}$, $c = 12.9470(18) \text{ \AA}$; $\alpha = 80.09(5)^\circ$, $\beta = 68.74(5)^\circ$, $\gamma = 67.86(5)^\circ$, $V = 1116.6(2)$, $Z = 1$.

A Mercury diagram is shown in Figure VII. The compound which crystallizes is a diferric, μ -oxo-bridged bicationic binuclear species, the ligand tetradently coordinating. The main metal-ligand distances and angles are given in Table III.

This structure is directly comparable with that obtained from the parent compound TPAFeCl₂, [8-22]. The two ligands are located trans to each other to the Fe-O-Fe segment. The tertiary amine of the ligand is located in the trans position of the coordinate chloride.

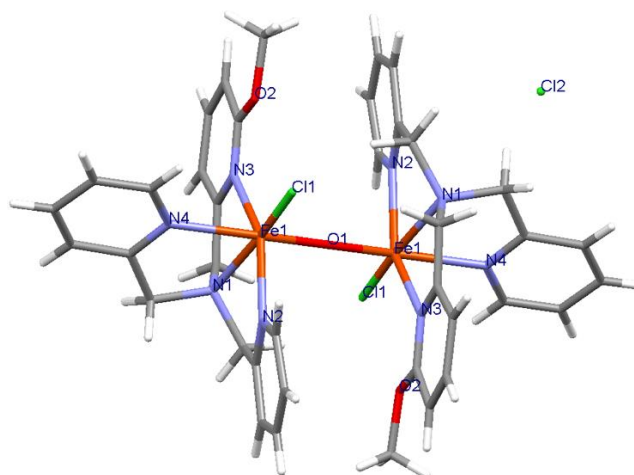


Figure VII : Mercury representation of the cation $[((\text{OMe})\text{TPAFeCl})_2\text{-O}]^{++}$

<u>(((MeO)TPAFeCl)₂O]⁺⁺</u>	
Distances	Angles
Fe1-O1=1.7947(19)Å	O1 Fe1 N2=94.0(3)° O1 Fe1 N1=93.1(3)° N2 Fe1 N1=75.0(5)°
Fe1-N2=2.167(12)Å	O1 Fe1 N3=88.0(3)° N2 Fe1 N3=151.2(5)°
Fe1-N1=2.205(12)Å	N1 Fe1 N3=76.2(5)° O1 Fe1 N4=167.0(3)°
Fe1-N3=2.209(13)Å	N2 Fe1 N4=91.5(4)° N1 Fe1 N4=77.0(4)°
Fe1-N4=2.229(10)Å	N3 Fe1 N4=81.6(4)°
Fe1-Cl1=2.307(4)Å	O1 Fe1 Cl1=100.71(12)° N2 Fe1 Cl1=93.6(4)° N1 Fe1 Cl1=162.8(3)°
O1-Fe1=1.7947(19)Å	N3 Fe1 Cl1=114.3(4)° N4 Fe1 Cl1=90.7(3)° Fe1 O1 Fe1=180.0°

Table III : Main metal-ligand distances and angles.

Reactivity in the presence of substrate.

The oxygenation mechanism of the complexes, shows that at some point an intermediate $\text{Fe}^{(\text{IV})}$ - oxo species is formed. This species is very oxidizing, during the reaction in the absence of substrate, it reacts with a complex molecule to form a μ -oxo diferric species. It would therefore be conceivable that such a species in the presence of a substrate, such as cyclohexane, is capable of transferring oxygen to lead to the formation of an oxidized substrate. It is with this hope that we carried out the following experiments.

The oxidation of cyclohexane to cyclohexanone has already been studied with, ferrous chloride salt, and complexes of TPA and we will compare the results with complexes substituted by methoxy groups. It is therefore a matter of reacting the three complexes with cyclohexane in the presence of O_2 . We used zinc amalgam as the $\text{Fe}^{(\text{III})}$ / $\text{Fe}^{(\text{II})}$ reducing agent to regenerate reactive species during the reaction. In a schlenck tube, prepare a solution of known concentration of complex dissolved in acetonitrile, add cyclohexane, a few drops of zinc amalgam, and bubble oxygen.

After one to two hours, a grayish solution is obtained, the acetophenone is added in a known quantity and the whole is filtered through Celite. Acetophenone is used as a reference for the analysis of GC gas chromatography results.

Results: the first signal appears at 4.1 minutes and corresponds to the acetonitrile peak, which is the most intense. Then a few seconds later follows the cyclohexane signal, a low intensity peak. At around 6.6 minutes, the appearance of cyclohexanone is observed, a very weak peak and at the end of 11.6 minutes the reference signal, acetophenone, appears. The relationship below makes it possible to calculate the concentration of cyclohexanone and therefore the TON turn over number:

$$[\text{cyclohexanone}] = 1.2 [\text{acetophenone}] * \text{Aire (cyclohexanone)} / \text{Aire (acetophenone)}$$

$$\text{TON} = [\text{cyclohexanone}] / [\text{catalyst}]$$

Below (Table IV) are listed the results obtained:

	FeCl ₂	TPAFeCl ₂	MeOTPAFeCl ₂
TON	=0.4	=8	=29

Table IV: the turnover of catalysis of conversion of cyclohexane to cyclohexanone

Conclusion

A series of TPA ligand substituted by methoxy groups was synthesized, characterized and complexed with FeCl₂. These types of ligand are the electrodonner ligands. The desire to create such a ligand is not trivial, in fact we are synthesized this ligand trying to demonstrate the defiant reactivity between electrodonner and the electro-deficient ligand, which has been study very will (as we know the more the metal center of the complex has a strong Lewis acid character, for a given geometry). This comparison will demonstrate the deferent speed of O₂ coordination on the complex. The complexe are then prepared and characterized by different spectroscopic techniques, thus making it possible to predict their geometry in solution and in the solid state for MeOTPAFeCl₂. The compound MeOTPAFeCl₂ exhibits equilibrium of mon and binuclear complexes in solid state and in solution.

This leads us to the study of the reactivity of the complexe in the presence of the substrate, cyclohexane. We have seen that this reaction was catalytic, indeed several cycles are observed.

The reaction is clean since it leads to the formation of a ketone and not an alcohol. From the results in Table II, we should have formed alcohol since we assumed the oxidizing species to be the intermediate Fe^(IV)-oxo. Thus, mechanistic studies are to be expected [17-27]. Objective: It is now imperative to improve the efficiency of this reaction, that is to say to limit the deactivation of the catalyst. The incorporation of the complex in a protective matrix: i solid (zeolite, nanotube), or biological polymer (protein), we would seem to be an effective way to remedy the problem.

Synthesis of ligands:

The synthesis of the DPA and TPA ligands was carried out according to published methods [1,2] No particular difficulty was encountered.

Synthesis of 2-methoxy-6-Methylpyridine [23]. :

6.10 g (153mmoles) of 60% NaH are washed with hexane and the mineral oil is extracted several times under argon until obtaining NaH without oil (pure NaH). 12 g (70mmoles) of 2-Bromo-6-Methylpyridine are dissolved in 80 ml of DMF, the solution is added to the NaH gradually over 15 minutes. The temperature of the medium is adjusted to 0 ° C using an ice bath under argon. The medium becomes very thick and the temperature does not exceed 0 ° C. 6.1 cm³ (153mmol) of methanol are added gradually over 5 minutes. The reaction mixture is refluxed for 3 hours at 80 ° C. The solution obtained is allowed to cool to room temperature. The product is extracted several times with ether. At the end, the transparent pale yellow solution obtained is washed several times with distilled water. Then, the organic phase is dried over MgSO₄ then filtered and evaporated. This transparent pale yellow liquid is distilled under reduced pressure (P = 15 mmHg). The fraction of the desired product was collected between 80 and 85 ° C, it is a colorless liquid.

RMN¹H, (CDCl₃, □□□, ppm) :7.35-7.31, (1H_γ, m) 6.62-6.60 (1H_β, d, J=6); 6.48-6.45 (1H_{β'},d, J=9); 3.86,(s, 3H,OCH₃); 2.28, (s, 3H,CH₃).

Synthesis of 2-methoxy-6-Bromomethylpyridine [23]:

Into a solution of 2-methoxy-6-methyl pyridine (12g, 97.5 mmoles) in 200ml of carbon tetrachloride CCl₄ are introduced 20.82 g of N-bromosuccinimide (117.3 mmoles) and 675 mg of azobisisobutyronitrile (2.79 mmoles). The reaction mixture is brought to reflux (90 ° C.) for 5 hours. At the end, the solution is evaporated to dryness. The product taken up in 200 ml of toluene. The precipitate which forms is filtered off and the yellow solution is concentrated. The product is purified by chromatography column on silica mounted in toluene. The separation is followed by thin layer chromatography (TLC). This is the third fraction that contains the desired product. The product 2-methoxy-6-Bromomethylpyridine is a transparent liquid obtained with a yield of 50% (mass obtained: 9.85 g)

RMN¹H : (CDCl₃, □, ppm) 7.54-7.47, (t,1H) 6.96-6.96 (d,1H); 6.64-6.61 (d,1H); 4.43, (s,2H); 3.91(s,3H).

Synthesis of Bis (pyridin-2-ylmethyl) amine (DPA) [24]:

5 g (39.2 mmoles) of picolyl chloride are dissolved in 120 ml of ethanol. 8.84 g (81.8 mmoles) of 2-aminomethylpyridine are then added. The reaction mixture is refluxed for 12 hours at 85 ° C. The solution obtained is taken up in an aqueous solution of K₂CO₃, then dichloromethane is added. The organic phase is then washed and then dried over MgSO₄, filtered and evaporated. The product is distilled under 1 to 2 mmHg and two fractions are collected: one distilling between 45 and 55 ° C (2-

aminomethylpyridine) and the other distilling between 139-141 ° C (Bis (pyridin-2-ylmethyl) amine) with an efficiency of 80%.

Synthesis of (bis (2-methylpyridine) [(6-methoxy-2-methylpyridine)] amine) (MeOTPA):

1 g (4.95 mmol) of 2-bromomethyl-6-methoxy-pyridine and 0.985 g (4.95 mmol) of DPA are introduced into a flask. 1 equivalent of Na₂CO₃ or 836 mg and approximately 150 ml of ethanol are added. The reaction mixture is refluxed for 14 hours at 95 ° C. The solution is evaporated and distilled water is added in order to solubilize the remaining Na₂CO₃, dichloromethane to solubilize MeOTPA. The medium is decanted, the recovered organic phase is dried over MgSO₄ and then filtered. The filtrate is then purified by chromatography on an alumina column mounted with DCM containing 7% methanol. MeOTPA has an orange-brown color (Yield: 1.346g = 85%).

Analyse élémentaire :

Calculated for C₁₉H₂₀N₄O. C : 71,23 ; H : 6,29 ; N : 17,49.

Calculated for (C₁₉H₂₀N₄O)₂+H₂O : C : 69,28 ; H : 6,43 ; N : 17,10.

Obtained for (MeOTPA)₂.H₂O . C : 69,27 ; H : 6,409 ; N : 16,56.

RMN ¹H (300 MHz, CDCl₃) : δ (ppm) 3,78 (s, 2H,CH₂); 3,85 (s, 4H,2xCH₂); 3,94 (s, 3H,CH₃) ; 6,53-6.50 (d, 1H) ; 6.97-7,001 (d, 1H) ; -7.03-7,10 (m, 2H) ; 7,40-7.50 (t, 2H) ; 7,55-7.62 (m, 3H) ; 7,74 (m, 1H) ; 8,46 (d, 2H, α-pyridine).

RMN ¹³C : 163(C-OMe) ; 159(2xC); 156(C) ; 148(2CH) ; 138(CH) ; 136(2CH) ; 122(2CH) ; 121(2CH) ; 115(CH) ; 108(CH) ; 60(2C,CH₂); 59(2 CH₂) ; 53(CH₃) .

Procedure for determining the molar conductivity of a complex.

The measurements are taken at 295K.

4 ml of degassed dry acetonitrile are introduced into the measuring cell, and the relative conductivity of the blank is measured (A). The relative conductivity of the sample dissolved in 4 ml of the same solvent is then measured (B). The conductivity of the compound is obtained by subtracting B – A. The molar conductivity is obtained by the ratio (B – A) / Complex concentration. In the case of Bis-catTPAFeCl₂, the ligand is first introduced into the cell. The metallation is carried out in situ, by adding a stoichiometric quantity of FeCl₂ which is excessively measured.

Common procedure for the metallation of all ligands with ferrous chloride.

The principle of this reaction is to oppose one equivalent of ferrous chloride to one equivalent of ligand. In practice, a slight excess of ligand (5 to 10%) is used: this allows complete complexation of the metal, and the excess ligand is easy to remove by washing with ether or THF.

This reaction takes place in the absence of Schlenck tube air. The solvents used are all distilled and degassed before use. The filtrations are carried out under overpressure by means of filter cannulas.

The standard procedure as published is shown below:

0.9 Equivalents of ferrous chloride in solution in THF are added by cannula to a solution of 1.0 equivalent of Ln ligand in THF. The color quickly turns to orange-yellow, and the reaction medium is kept under stirring for at least 2 hours at room temperature.

The solvent is then evaporated in vacuo and the complex extracted with acetonitrile. After filtration and concentration, a yellow-orange solid is obtained by slow addition of diethyl ether. The solid thus obtained can be recrystallized by adding ether to a solution in acetonitrile.

After drying with a vacuum pump, the solid is characterized by different techniques. The yields of own products are between 85 and 90%.

General method for the oxidation of cyclohexane:

5 cm³ of acetonitrile and 270 μ L of cyclohexane are introduced into a Schlenck tube, which are degassed and then 0.005 mmol of the complex is dissolved therein. One to two drops of zinc amalgam are then added, the whole is kept under stirring. The oxygen in a flask is then gradually added to the solution. One to two hours is enough for the mixture to become cloudy, this indicates that the catalyst precipitates at the bottom of the Schlenck tube, the reaction is complete. 4.9 μ L of acetophenone are added to the solution and the whole is filtered through Celite. Gas chromatographic analysis follows.

Referances

1. Machkour A, Thallaj NK, Benhamou L, Lachkar M, Mandon D. *Chemistry*. 2006 Aug 25;12(25):6660-8. P 6660-6661-6662-6663.
2. Thallaj, N., Machkour, A., Mandon, D., Welter, R., *New. J. Chem.*, 2005, 29, 1555 – 1558.
3. Thallaj, N. K. *Damascus University Journal for Basic Sciences*. 34 (1) 2018.
4. Thallaj. N. K. *Journal of AlBaath University* (39) 2017.
5. Thallaj. N. K. *Tishreen University Journal for Research and Scientific Studies* 38 (6) 2016.
6. Thallaj NK, Rotthaus O, Benhamou L, Humbert N, Elhabiri M, Lachkar M, Welter R, Albrecht-Gary AM, Mandon D. *Chemistry*. 2008;14(22):6742-53. P6745-6746-6747..
7. Wane A, Thallaj NK, Mandon D. *Chemistry*. 2009 Oct 12;15(40):10593-602. P10594-10595-10595.
8. Thallaj NK, Orain PY, Thibon A, Sandroni M, Welter R, Mandon D. *Inorg Chem*. 2014 Aug 4;53(15):7824-36. P7826-7827-7828.
9. N. K. Thallaj, J. Przybilla, R. Welter and D. Mandon, *J. Am. Chem. Soc.* 2008, 130, 2414-2415.
10. N. K. Thallaj, D. Mandon and K. A. White, *Eur. J. of Inorg. Chem.*, 2007, 44–47.
11. N. K. Thallaj, A. Machkour, D. Mandon and R. Welter, *New J. Chem.*, 2005, 29, 1555–1558.

12. Thallaj, N.; International journal of applied chemistry and biological sciences 2021, 2 (4), 65-77.
13. Thallaj, N.; Indian Journal of Advanced Chemistry (IJAC)2021, 1 (2), .
14. Thallaj, N.; International Journal of Research Publication and Reviews (IJRPR)2021, 2, 10, 951-959
15. L. Labban, N. Thallaj, Z. Malek; International Journal of Medical Studies, 2020, 5, No 12, 23-36.
16. L. Labban, M. Kudsi, Z. Malek, N. Thallaj; Advances in Medical, Dental and Health Sciences, 2020,3, 3,45-48.
17. L. Labban, N. Thallaj, M. Al Masri; Journal of Advanced Research in Food Science and Nutrition, 2020,3,1,34-41.
18. Thallaj, N; agha, M. I ,H;, nattouf; A.H; katib, CH; karaali, A; Moustapha, A; Labban L;open access library journal, 2020,7,5,1-21.
19. L. labban; N. thallaj; A. labban; archives of medicine, 2020, 12, 2:8, 1-5.
20. L. labban; N. thallaj; international journal of herbal medicine,2020, 8, 2, 33-37.
21. L. Labban, N. Thallaj, Z. Malek; Journal of Medical Research and Health Sciences, 2019, 2, 11, 784-787.
22. L. labban N. Thallaj; acta scientific nutritional health, 2019, 3,10, 7-12.
23. Malek, Z.S.; Sage D.; Pevet, P.; Raison, S.; Endocrinology 2007, 148 (11), 5165-5173.
24. Malek, Z.S.; Dardente, H.; Pevet, P.; Raison, S.; European Journal of Neuroscience 2005, 22 (4), 895-901.
25. Malek, Z.S.; Pevet, P.; Raison, S.; Neuroscience 2004, 125 (3), 749-758.
26. Malek, Z.S.; Labban, L.; The International Journal of Neuroscience, 2020, 1-7.
27. Malek, Z.S.; Labban, L.; European Journal of Pharmaceutical and Medical Research 2019, 6 (11), 527-532.
28. Malek, Z.S.; Journal of AlBaath University 2018, 40 (4), 39-62.
29. Malek, Z.S.; Tishreen University Journal for Research and Scientific Studies, 2018, 40.
30. ZS Malek, LM Labban; International Journal of Neuroscience, 2021,131 (12), 1155-1161.
31. ZS Malek, LM Labban; Journal of current research in physiology and pharmacology, 2020, 4, (1),1-5.
32. L.M. Labban, M. M. Alshishkli, A. Alkhalaf, Z. Malek; J. Adv. Res. Dent. Oral Health, 2017, 2(3&4), 1-4.
33. L Labban, ZS Malek, Open Access Library Journal, 2018, 5 (07), 1-11.
34. L Labban, ZS Malek, Ann Food Nutr Res J, 2019,1 ,1
35. Labban, L. and N. Thallaj, 2019. Acta Scient. Nutr. Health, 3: 7-12.
36. V. Caprio, J. Mann, J. Chem. Soc., Perkin Trans. 1, 1998, 3151–3155.